AD-A110 796 NAVAL POSTGRADUATE SCHOOL MONTEREY CA F/G 21/5
COMBUSTION BEHAVIOR OF SOLID FUEL RAMJETS. VOLUME II. EFFECTS O--ETC(U)
AUG 81 M E METOCHIANAKIS, W V GOODWIN, U KATZ
UNCLASSIFIED NPS67-81-011 NL

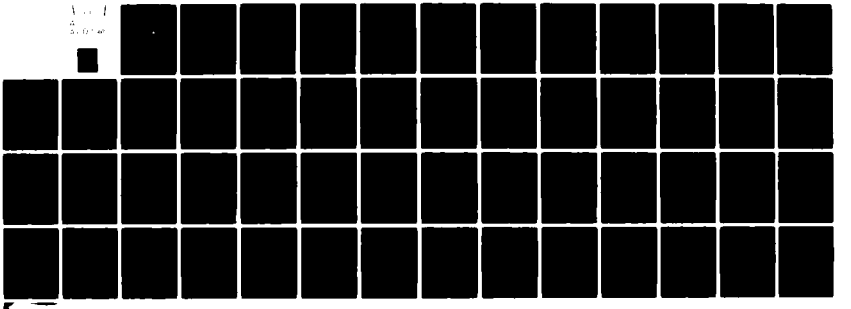

END
DATE FILMED
3 82
DTIC

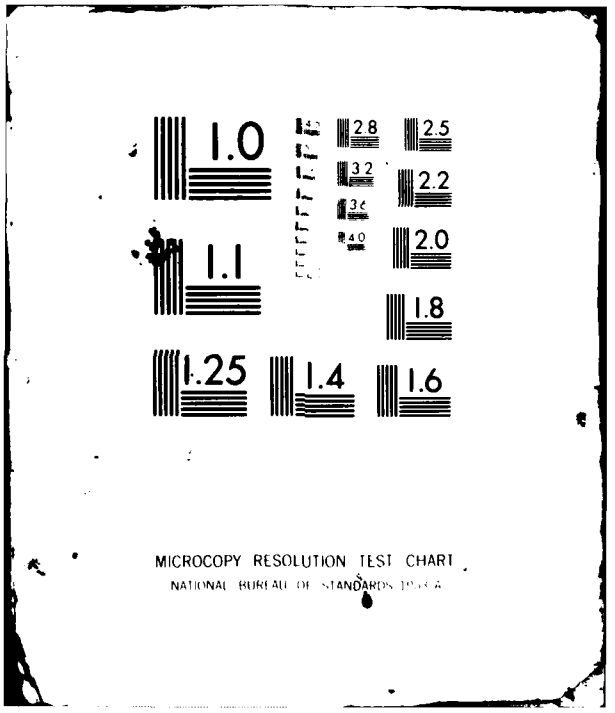
1.0
1.1
1.25
1.4
1.6
1.8
2.0
2.2
2.5
2.8
3.2
3.6
4.0
MICROCOPY RESOLUTION TEST CHART
NATIONAL BUREAU OF STANDARDS 1963-A

(2) LEVEL III

NPS67-81-011

AD A110796

NAVAL POSTGRADUATE SCHOOL

Monterey, California

COMBUSTION BEHAVIOR OF SOLID FUEL RAMJETS

VOL II. EFFECTS OF FUEL PROPERTIES AND FUEL-AIR MIXING ON COMBUSTION EFFICIENCY

Michael E. Metochianakis, William V. Goodwin
Uri Katz, and David W. Netzer

August 1981

Prepared for:

Naval Weapons Center
China Lake, CA 93555

NAVAL POSTGRADUATE SCHOOL
Monterey, California

Rear Admiral J. J. Ekelund
Superintendent

D. A. Schrady
Acting Provost

The work reported herein was supported by the Naval Weapons Center, China Lake, CA.

This report was prepared by:

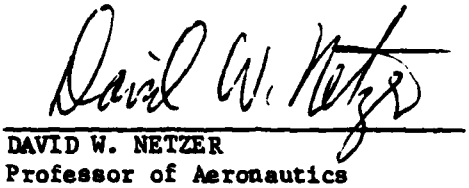

DAVID W. NETZER
Professor of Aeronautics

Reviewed by:

M. F. PLATZER
Chairman of Aeronautics

Released by:

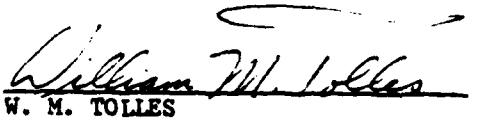

W. M. TOLLES
Dean of Research

SECURITY CLASSIFICATION OF THIS PAGE (When Data Entered)

REPORT DOCUMENTATION PAGE		READ INSTRUCTIONS BEFORE COMPLETING FORM
1. REPORT NUMBER NPS67-81-011	2. GOVT ACCESSION NO. AD-A110796	3. RECIPIENT'S CATALOG NUMBER
4. TITLE (and Subtitle) Combustion Behavior of Solid Fuel Ramjets Vol II. Effects of Fuel Properties and Fuel-Air Mixing on Combustion Efficiency		5. TYPE OF REPORT & PERIOD COVERED Final 1981 6. PERFORMING ORG. REPORT NUMBER
7. AUTHOR(s) David W. Netzer		8. CONTRACT OR GRANT NUMBER(s)
9. PERFORMING ORGANIZATION NAME AND ADDRESS Naval Postgraduate School Monterey, California 93940		10. PROGRAM ELEMENT, PROJECT, TASK AREA & WORK UNIT NUMBERS N6053081WR30137
11. CONTROLLING OFFICE NAME AND ADDRESS Naval Weapons Center China Lake, CA 93555		12. REPORT DATE August 1981 13. NUMBER OF PAGES 45
14. MONITORING AGENCY NAME & ADDRESS(if different from Controlling Office)		15. SECURITY CLASS. (of this report) UNCLASSIFIED 15a. DECLASSIFICATION/DOWNGRADING SCHEDULE

16. DISTRIBUTION STATEMENT (of this Report)

Approved for public release; distribution unlimited

17. DISTRIBUTION STATEMENT (of the abstract entered in Block 20, if different from Report)

18. SUPPLEMENTARY NOTES

19. KEY WORDS (Continue on reverse side if necessary and identify by block number)

Solid Fuel Ramjet
Fuels
Combustion Efficiency

20. ABSTRACT (Continue on reverse side if necessary and identify by block number)

Fundamental SFRJ fuel properties were determined using a DTA and a gas chromatograph for both high and low heating rates. The performance of these fuels was then measured under various operating conditions and test geometries. Fuel properties were found to have some effect on the obtainable combustion efficiency but much larger effects could be induced by the flow conditions (induced mixing near the fuel surface, bypass air, etc.).

DD FORM 1473 EDITION OF 1 NOV 65 IS OBSOLETE
S/N 0102-014-6601

UNCLASSIFIED
SECURITY CLASSIFICATION OF THIS PAGE (When Data Entered)

TABLE OF CONTENTS

LIST OF FIGURES

LIST OF TABLES

SYMBOLS

A	area
A^*	nozzle throat area
f/a	fuel-air ratio
D_i	initial inside diameter of fuel grain
F	thrust
g_c	32.2 lbm-ft/lbf-sec^2
G	mass flow per unit area
L	Fuel grain length
M	Mach number
$\dot{m}$	mass flow rate
P	pressure
P_c	combustion pressure
P_t	stagnation pressure
R	gas constant
$\dot{r}$	average fuel regression rate
t_b	burn time
T	temperature
ΔW_f	weight change of fuel grain
γ	ratio of specific heats
$\eta_{\Delta T}$	temperature rise combustion efficiency
ϕ	equivalence ratio = $\frac{(f/a)}{(f/a)_{stoichiometric}}$

Subscripts

a	air, ambient conditions
c	combustion chamber
ex	experimental
f	fuel
H	head-end of motor
p	primary air
s	secondary (bypass) air
t	stagnation
T	Total (primary + bypass) air + fuel ($\dot{m}_p + \dot{m}_s + \dot{m}_f$)
4	nozzle inlet

I. INTRODUCTION

The Naval Postgraduate School has had a continuing research effort directed at the combustion behavior of solid fuel ramjets under the sponsorship of the Naval Weapons Center, China Lake. Both mathematical modeling [Refs. 1-3] and experimental efforts [Refs. 4-9] have been conducted to determine the effects of design variables on the obtainable performance. One major area requiring additional attention is the attainment of improved combustion efficiency together with higher energy fuels.

New fuels are required which will yield high density impulse and good flammability limits for various inlet, grain and aft mixing chamber configurations. Recently a wide variety of HTPB based fuels have been considered [Ref. 10 & 11]. To date the alternate fuels have not yielded significant performance improvements and indications are that mixing processes within the fuel grain port may be as important as fuel composition. The attainment of higher efficiencies with existing or new fuels may require innovative methods for controlled mixing of the diffusion limited combustion processes within the fuel port. However, there is some evidence from past work at NPS that variation in the curing process of Plexiglas has resulted in significant changes in combustion efficiency without additional mixing being attempted. Additional work is required to better understand the effects of fuel properties and mixing on the attainable combustion efficiency.

Cold flow tests at UTC/CSD and NPS have been used for model validation efforts and to better understand the flowfield within the fuel grain and aft mixing chamber. However, these data have not been consistently

related to fuel performance (regression pattern, efficiency, flammability limits, etc.) in a reacting environment.

It would be most beneficial if cold flow measurements and fuel characteristics could be used a priori to predict the expected fuel behavior in a reacting environment and in a specific geometric configuration.

In this investigation the performance of several fuels was measured under various operating conditions and test geometries and an attempt was made to correlate the results with cold flow measurements, fundamental fuel characteristics, and/or the amount of mixing induced near the fuel surface.

In Volume I of this report combustion performance was determined for Plexiglas fuel grains using various operating conditions and motor geometries, and an attempt was made to correlate the results with measurements made in nonreacting flows. Conclusions of that investigation were:

1. Geometric changes to the solid fuel ramjet which result only in increased core-flow turbulence do not significantly affect fuel regression rate or combustion efficiency.

2. Non-reacting flow measurements of near-wall turbulence "intensity" profiles appear to reasonably correlate with measured fuel regression profiles in the reacting environment.

3. Utilization of grooves in the surface of PMM fuel grains increased near-wall turbulence in the head-end of the fuel grain but did not affect combustion efficiency (with low air flow rates).

4. If enhanced/controlled mixing within the fuel port is to result in increased combustion efficiency it probably will have to be introduced very close to the diffusion flame zone.

5. Bypass air has more effect on the flow upstream (within the fuel port) as the inlet step height is decreased.

6. Combustion pressure oscillations appear to be the result of induced disturbances to the shear layers that are present at the entrance sections of the fuel grain and the aft mixing chamber.

The present investigation had the following objectives:

1. Determine if significant differences in fuel properties can result in differences in combustion efficiency or the dependence of combustion efficiency on equivalence ratio.

2. Determine how enhanced mixing near the fuel surface affects the combustion efficiency of HTPB based fuels.

II. METHOD OF INVESTIGATION

The investigation consisted of four related studies; determination of (1) fundamental chemical properties of solid fuels for ramjets, (2) the obtainable combustion efficiencies from these fuels, (3) the effects of near-wall mixing, and (4) the variation of combustion efficiency with equivalence ratio for Plexiglas fuel grains.

Thirteen fuel compositions were investigated (Table I); the Naval Weapons Center (NWC) provided fuels 1 through 10 whereas the United Technologies Corporation, Chemical Systems Division (UTC/CSD) provided fuels 11 and 12.

Using the differential thermal analyzer (DTA) with a heating rate of 100°C/min, each fuel sample was tested in a nitrogen atmosphere and its thermal behavior examined in the range from 22°-500°C.

Gases emitted during the DTA tests (at phase transitions) were inserted into a gas chromatograph in order to determine the approximate molecular weights. Since the heat fluxes in the actual combustion environment are high compared with the maximum DTA heating rate of 100°C/min, an argon laser was also used to pyrolyze the fuel samples and produce the gases for the gas chromatograph.

Those fuels which had significantly different DTA characteristics were fired in a ramjet combustor (Fig. 1) to determine if the fuel properties could be correlated with obtainable performance. Four fuels were tested under three different types of mixing processes within the combustor: no bypass, no bypass with circumferential grooves cut in the fuel grain, and 50% bypass.

TABLE I

FUEL SAMPLE COMPOSITION

ITEM NO.	DESCRIPTION
1	HTPB/CLPS
2	HTPB/Binor-S
3	HTPB/Magnesium
4	HTPB/RJ-4
5	HTPB/Diamantane
6	HTPB/CPD Oligomers
7	HTPB/RJ-4/RJ-5
8	R45 HT/DDI
9	R45 M/DDI
10	R45M/TDI
11	Uncured Zecorez
12	Cured Zecorez
13	Plexiglas (PMM)

Additional tests were conducted using Plexiglas (PMM). Fuel grain length was varied to produce a wide variation in equivalence-ratio. Combustion efficiencies from these grains were determined for both the non-bypass and the bypass configurations. The combustion efficiencies of these grains were then compared to the combustion efficiencies of cylindrically perforated grains of varying lengths that also had internal grooves machined into them (Fig. 2). The latter tests were made to provide additional data on the effects of near-wall mixing on combustion

efficiency. Similar tests had been previously made using only one fuel grain length. Firings were also made in which the aft mixing chamber was almost eliminated. These tests were made to determine what percentage of the combustion occurred aft of the fuel grain.

III. DESCRIPTION OF APPARATUS

A. DIFFERENTIAL THERMAL ANALYZER (DTA)

The differential thermal analyzer used was a DUPONT 900 model with a temperature range from -100°C to 500°C and a heating rate capability from 1°C to 100°C per minute.

The standard cell assembly contained the heating block, heater, thermocouples and thermal shield. These were contained within a bell jar which was positioned with quick-acting hold downs. The cell was provided with connections for purging, cooling and evacuation and was also removable from the analyzer.

A heating block was used which contained four wells; a central large one for the cartridge heater and three smaller ones for the controlling, sample and reference thermocouples within 4mm glass tubes.

Nitrogen was used as the inert gas for purging the cell.

B. GAS CHROMATOGRAPH

The gas chromatograph used was a BENDIX CHROMALAB SERIES 2200. A linear temperature programmer could be used to control the temperature in the range from 0°C to 500°C. It featured two adjustable rates of rise (0-50°C/min) and three adjustable hold times (0-50 minutes) at three temperatures.

The columns used were SE 30 20% (active material) - Chromosorb 60/80 (packing material-stationary phase).

Helium was used as the carrier gas because of its high thermal conductivity. The thermal conductivity detector was used because of the difference between the thermal conductivity of pure carrier gas and the carrier gas-sample gas mixture, and also because of the ability to detect almost any organic or inorganic compound.

The gases were withdrawn from the sample tubes in the DTA and injected into the gas chromatograph using a gas-tight HAMILTON syringe. The chromatograms were traced by a strip-chart recorder (SARGENT, MODEL TR) connected to the output of the detector-amplifier unit.

C. ARGON LASER

The laser used was a CONTROL LASER, MODEL 902, ARGON type with a maximum current of 33A and a maximum power at 4880A° of 0.9 watts. A biconvex lense with a focal length of 11.5 cm was used to focus the laser beam on the fuel sample. The maximum current used during the runs was 29A.

D. RAMJET MOTOR

A schematic of the solid fuel ramjet apparatus is shown in Figure 1 and was that previously used by Mady, and others, at the Naval Postgraduate School [Refs. 4, 6-9] and described in Volume I of this report. The motor consisted of four sections: the head-end assembly, the step insert section, the fuel grain and the aft mixing chamber with a converging nozzle.

The head-end assembly contained the air inlets, the inlet for the ignition ethylene, the nitrogen purge and the cooling air inlets.

The step insert section was 7 cm long and held the step in place. A 1.91 cm diameter (for HTPB) or a 1.27 cm diameter (for PMM) inlet was used to provide the sudden expansion into the 3.81 cm diameter fuel grain port. An orifice was used at the aft end of the fuel grain to maintain a fixed area ratio between the fuel port and the aft mixing chamber.

Fuel grains used were HTPB (Hydroxy-Terminated Polybutadiene) (supplied by the Naval Weapons Center (NWC), China Lake and the United Technologies Corporation (UTC/CSD)), HTPB/RJ-4, and cast Plexiglas.

The bypass air was dumped into the aft mixing chamber through two 2.07 cm diameter ports perpendicular to the motor centerline. These two dump ports were located 180° apart, and just aft of the mixing chamber recirculation zone (4.53 cm aft of the fuel grain).

In some of the 15.2 cm length grains the internal surface was grooved (ridged) in an attempt to increase fuel-air mixing within the fuel port (Fig. 2).

The exhaust nozzle used was converging with a 2.05 cm (for HTPB and HTPB/RJ-4 fuels) or a 1.191 cm (for plexiglas) throat diameter.

IV. EXPERIMENTAL PROCEDURES

A. DETERMINATION OF PHASE CHANGES OF FUEL SAMPLES

The differential thermal analyzer (DTA) was used to determine where phase changes occurred for various heating rates. Prior to running of the tests, the DTA was calibrated using reference material (Al_2O_3) in both sample and reference positions of the heating block, and a flat base line was obtained.

Each fuel sample was cut into very small pieces and ten (10) mg of that powder like sample was mixed with twenty (20) mg of aluminum oxide (Al_2O_3). The purpose of the sample dilution was to obtain a better match in thermal conductivity between the sample and reference materials [Ref. 12 & 13]. The 30 mg mixture (20 mg Al_2O_3 and 10 mg fuel) was put into a 4mm diameter capillary tube which was inserted into the proper well of the heating block (sample position). Another 4mm tube with 30 mg Al_2O_3 was put into the reference well of the heating block. A third 2mm diameter capillary tube, filled with glass beads to a depth of 3mm, was placed in the remaining well of the heating block (control position). One Cr-Al thermocouple was then inserted into each tube with its junction immersed in the sample.

The cell assembly was then put in place on the DTA and the following settings in the recorder controls were made: (a) temperature ZERO SHIFT at zero, (b) temperature SCALE at 100°C/min, (c) temperature differential SCALE at 50°C/min, and (d) BASELINE SHIFT at -1.

The cell assembly was then repeatedly evacuated and purged with nitrogen three times to ensure that the sample was in a nitrogen atmosphere during the heating process.

B. GENERATION OF GASES FOR THE GAS CHROMATOGRAPH

1. Low Heating Rate

The gas samples produced using a low heating rate were obtained using the DTA. A different bell jar was used in this case in order to allow the sample gases to be removed using the air-tight syringe.

Each fuel sample was cut into small pieces, but in this case was not diluted with a reference material. Fifty (50) mg of fuel sample were put into a 4mm diameter capillary tube. Then a 2mm diameter tube (open on both ends) and a Cr-Al thermocouple were inserted into the 4mm tube. This was accomplished such that the thermocouple junction and one end of the 2mm tube were immersed in the fuel sample. An air-tight syringe was passed through a septum in the jar and then inserted into the 2mm tube inside the jar. A 4mm tube with 50 mg Al_2O_3 as reference material and a 2mm tube with glass beads (3mm deep) together with the corresponding thermocouples were also put in the proper wells of the heating block.

The cell assembly was then put in place and the same settings were made as used for determining the phase changes. It was then evacuated and purged with nitrogen three times and the heating rate was set to 100°C/min. As soon as a phase change was completed a sample of the gases emitted was pulled off with the syringe and injected into the gas

chromatograph in order to determine the approximate distribution of molecular weights.

2. High Heating Rate

The gas samples obtained with a high heating rate were generated using a focused Argon-ion laser. The output power of the laser was 0.7 watts, but after the beam passed through the lense the power was reduced to 0.4 watts. The heat flux of the laser beam at the fuel sample surface was approximately 7.3×10^{5} $\frac{\text{Joules}}{\text{m}^2\text{-sec}}$, while typical convective fluxes in the actual combustion environment are 6×10^{5} $\frac{\text{Joules}}{\text{m}^2\text{-sec}}$.

A piece of fuel was put into a small glass container which was sealed on the top with tape. The fuel surface was positioned at the focal point of a biconvex lense. The beam was then directed and focused on the fuel sample which instantaneously pyrolyzed. A small sample of the emitted gases was collected using an air-tight syringe. The gases were then injected to the gas chromatograph for the molecular weight determination.

C. DETERMINATION OF THE APPROXIMATE MOLECULAR WEIGHTS OF THE PYROLYZED FUEL SAMPLES

A gas chromatograph (BENDIX, CHROMALAB 2000) was used to determine the approximate distribution of molecular weights of the gases emitted from the fuel samples when subjected to low and high heating rates. The helium carrier gas was provided to the gas chromatograph at a pressure of 2.67 atmospheres and the flow rates in both flow meters were set to 30cc/min. The inlet temperature was set at 150°C, whereas the thermal conductivity detector was set at 275°C. The linear temperature programmer which controlled the oven temperature was programmed to follow the sequence

as shown in Figure 17, where T_1=50°C was the initial temperature of the oven. The heater, blower and oven were turned on and allowed to stabilize for approximately two hours. A check was then made to verify that all temperatures were at equilibrium and then the thermal conductivity detector was turned "on". The bridge current was set at 200 ma.

For calibration purposes, the attenuation was set to the highest expected value and the recorder zeroed. The same procedure was repeated to consecutively lower attenuations and finally the attenuation was returned to the desired value. Before inserting the gases emitted during the pyrolysis, a run was made without injecting anything. This resulted in a flat and straight base line and insured that the gas chromatograph was free of any contaminants from earlier tests. The gases were then injected and the programmed temperature sequence was initiated.

After the runs of the fuels through the gas chromatograph some known samples (standards) were also injected. This was done in order to make a qualitative comparison between the retention times of the unknown samples and those of the standards. The standards used were: Pentane (C_5H_{12}), Hexane (C_6H_{14}), Heptane (C_7H_{16}), Nonane (C_9H_{20}), Decane ($C_{10}H_{22}$) and Dodecane ($C_{12}H_{26}$).

D. REACTING FLOW EXPERIMENTS (HOT FIRINGS)

All tests were performed in the SFRJ facilities of the Naval Postgraduate School. A schematic of the SFRJ motor is shown in Figure 1. The majority of the tests for other than PMM fuel grains were made using a nominal inlet air temperature of 340°K or 440°K. To heat the air to

that temperature, a non-vitiated air heater was used.

Nominal port air flow rates for fuels other than PMM were 240 gm/sec (G=21.05 gm/cm^2-sec) for non-bypass runs and 120 gm/sec (G=10.53 gm/cm^2 sec) for bypass runs. PMM required a smaller air inlet diameter which limited the air flow rate to a nominal value of 100 gm/sec. A bypass dump diameter of 2.07 cm was employed. All bypass tests were conducted with 50% of the air bypassed to the aft mixing chamber.

The inside diameter, length and weight of the fuel grains were measured before mounting in the motor. The ignition lasted for approximately 2 seconds and the combustion for 10 to 45 seconds. The motor was extinguished at the end of each run by simultaneously venting the air to the ambient and actuating a nitrogen purge system. Low pressure air was then blown through the motor for cooling. After each run, the inside diameter of the aft end and the weight of the fuel grain were measured again. The average regression rate was then calculated based on the weight loss and the burn time of the run.

Temperature rise combustion efficiency was calculated for each test using the formula:

$$\eta_{\Delta T} = \frac{T_{t_{ex}} - T_{t_{air}}}{T_{t_{th}} - T_{t_{air}}} \qquad (1)$$

The inlet stagnation temperature ($T_{t_{air}}$) was measured, and the "actual" combustor stagnation temperature ($T_{t_{ex}}$) was calculated from the following formula (isentropic, choked flow):

$$T_{t_{ex}} = \left(\frac{\gamma g_c}{\mathcal{R}}\right) \left[\left(\frac{2}{\gamma+1}\right)^{\frac{\gamma+1}{\gamma-1}}\right] \left[1+\frac{\gamma-1}{2} M_4^2\right] \frac{2\gamma}{\gamma-1} \left[\frac{P_c A^*}{\dot{m}_T}\right]^2 \qquad (2)$$

In this equation P_c and $\dot{m}_T$ were measured and γ and R were obtained from equilibrium calculations at the experimentally determined fuel-air ratio.

The ideal (theoretical) combustion temperature was also found from equilibrium calculations using the NWC PEPCODE program.

V. RESULTS AND DISCUSSION

A. DTA RESULTS

1. Introduction

The differential thermal analyzer (DTA) was used to determine where fuel composition changes occurred. The majority of the fuels investigated (Table I) were HTPB based fuels (Fuels 1 to 10) supplied by the NWC. The results obtained are presented in Figures 3 through 16. The general characteristic of the thermograms obtained for these polymers was that the transitions took place over a broad range of temperatures, rather than at one distinct temperature as is characteristic of pure materials.

2. HTPB/CLPS

HTPB/CLPS is an HTPB type fuel and had a broad exotherm (Fig. 3) with a peak occurring at approximately 422°C. The exothermic behavior was not anticipated. It could have resulted from a phase transition, such as crystallization of the polymer, or possibly from a reaction with an active gas (surface reaction). There was also a difference in the base line before and after the exotherm because of a loss of material. A weak endotherm followed the exotherm at approximately 490°C.

To further investigate the nature of the exothermic effect a sample of uncured (liquid) R-45M with AO was examined using the same DTA procedures. The thermogram of Figure 4 was obtained. It can be seen that this uncured liquid material, whose postfired composition was solid, produced an exotherm at exactly the same temperature as for HTPB/CLPS. This

indicated that the exothermic behavior at 422°C was primarily a property of the HTPB polymer.

3. HTPB/Binor-S

The Binor-S fuel (Fig. 5) resulted in a small endotherm at 322°C followed by an exotherm at 422°C. The exothermic behavior at 422°C was apparently due to the HTPB polymer, whereas the endotherm was probably due to phase transition of the Binor-S.

4. HTPB/Magnesium

This fuel had almost the same thermal behavior as the HTPB/CLPS material in the temperature range between 0°C and 500°C (Fig. 6). It also had the "characteristic" 422°C exotherm for HTPB.

5. HTPB/RJ-4

The HTPB/RJ-4 (Fig. 7) had significantly different characteristics from the previous fuels. It produced a very strong exotherm at a relatively low temperature (T = 190°C). This was apparently due to the RJ-4 material and may be attributed to some crystallization process [Ref. 13] or to a further polymerization [Ref. 14]. It also had a very broad and weak exotherm at 422°C, attributed again to HTPB.

6. HTPB/Diamantane

This fuel also had different characteristics from the other fuels (Fig. 8). It had three endotherms and the "characteristic" exotherm at 422°C due to HTPB. The first two endotherms occurred at low temperatures of 150°C and 180°C. Endotherms at low temperatures have been attributed to the fusion of the polymer and to the depolymerization reactions [Ref. 14]. The third endotherm occurred at 308°C and was probably the phase transition of the Diamantane.

7. HTPB/CPD Oligomers

The thermal behavior of this fuel is depicted in Figure 9. It had one exotherm at approximately 200°C (probably due to further polymerization), one endotherm at 325°C attributed to the CPD oligomers and the usual exotherm at 422°C due to HTPB.

8. HTPB/RJ-4/RJ-5

This fuel (Fig. 10) exhibited similar DTA characteristics to the HTPB/RJ-4, the difference being that the exothermic peak occurred earlier at a temperature of 159°C. The heat released during that exothermic reaction was less than for HTPB/RJ-4 fuel, resulting in a weaker exotherm. There was also a very broad exotherm at 422°C due to HTPB.

9. R45 HT/DDI

The thermal behavior of this fuel (Fig. 11) was similar to that of fuels 1, 2 and 3 (Table I) with second order transition at 260°C and a sharp exothermic behavior at 422°C, attributed again to the large HTPB content. The second order transition as evidenced by a baseline shift is not associated with latent heat, but rather with sudden changes in specific heat [Ref. 13].

10. R45 M/DDI

This fuel (Fig. 12) had the same behavior as that of the R45 HT/DDI fuel with the "characteristic" exothermic behavior at 422°C due to the R45M and the endotherm at 490°C, probably due to melting of the polymer.

11. R45M/TDI

The R45M/TDI fuel (being rich in HTPB content) had thermal

behavior similar to fuels 1, 2, 3, 8 and 9 (Table I) with the usual exotherm at 422°C, but no endotherm at 490°C (Fig. 13).

12. Uncured Zecorez

This fuel (supplied by the UTC/CSD) had a very shallow endotherm at 140°C and another broad endotherm with a peak at 360°C (Fig. 15).

13. Cured Zecorez

The cured zecorez had no phase transitions to 500°C, except a second order transition at 340°C and probably a weak exothermic effect at 475°C (Fig. 16).

14. PMM

The PMM fuel had a weak exotherm at 350°C, probably due to further polymerization, and a strong endotherm at 422°C due to melting or boiling phase transition of the polymer (Fig. 14).

15. Summary of Results

In summary, all HTPB based fuels (1, 2, 3, 8 and 10 in Table I) exhibited almost the same thermal behavior to 500°C with an exothermic peak at 422°C. The HTPB/RJ-4 fuel had significantly different characteristics from the previous fuels, producing a strong exotherm at low temperatures (T = 190°C) and a broad exotherm at 422°C due to HTPB content. The HTPB/Diamantane had different behavior from the other HTPB based fuels giving three endotherms followed by the HTPB exothermic characteristic. The PMM also had different characteristics from the above fuels producing a strong endotherm at 422°C due to melting or boiling phase transition of the polymer. Four of the above fuels (HTPB/CLPS, HTPB/RJ-4, HTPB/Diamantane and PMM), having significantly different DTA characteristics, were selected for the gas chromatograph tests (determination of the approximate molecular weights).

B. GAS CHROMATOGRAPH RESULTS

1. Introduction

To determine the approximate molecular weights of the combustion products, gases had first to be generated and then injected into the gas chromatograph. The DTA was also used to produce these gases for each fuel, using a heating rate of 100°C/min. However, since the heat fluxes in the actual combustion environment are much higher (typical value: $6 \times 10^5 \frac{\text{Joules}}{\text{m}^2\text{-sec}}$) than those provided by the DTA, an argon laser was also used to pyrolyze the fuel with a heat flux approximately $7.3 \times 10^6 \frac{\text{Joules}}{\text{m}^2\text{-sec}}$. The results from the gas chromatograph for the low (DTA) and high (laser) heating rates are presented in Figures 17 and 18 respectively.

2. Low Heating Rate (DTA)

The gases emitted during the DTA tests using a heating rate of 100°C/min were withdrawn and injected into the gas chromatograph using a gas tight syringe. The method of withdrawing and injecting the samples probably had some limitations since some reactions may continue even after the withdrawing and others may be quenched in the removal process.

Four fuels were investigated which had significantly different DTA characteristics. These fuels were: PMM, HTPB/CLPS, HTPB/RJ-4 and HTPB/Diamantane. The results obtained are shown in Figure 17. The traces of the known standards are also shown in the same figure.

The PMM resulted in a distinct peak at an oven temperature of 70°C and with a retention time of approximately 7 minutes. Comparing that retention time with the retention time of the Heptane (≈7.5 min, molecular

weight of 100) it can be said that the average molecular weight of the gases emitted during the pyrolysis of PMM was close to that of the monomer ($C_5H_8O_2$). The height of the chromatographic peak is proportional to the amount of sample gases injected.

In Figure 17 it is also observed that the HTPB/CLPS started passing through the detector after approximately 7.5 minutes from injection. Gases continued through the detector with increasing time to produce a maximum at 15 minutes, with a molecular weight approximately the same as that of decane (142). Two further peaks occurred at 27 and 30 minutes (oven temperatures 240° and 242°C) with average molecular weights greater than that for dodecane ($C_{12}H_{26}$).

The HTPB/RJ-4 had almost the same pattern as for HTPB/CLPS but in larger scale. The peaks were more distinct at corresponding points and it also started coming out of the column earlier. The first to come out was at approximately 2 minutes from the injection. At the third minute one larger peak occurred, corresponding to a molecular weight of approximately the same as that of Hexane (86). Then some distinct peaks occurred at times of 6, 9 and 12 minutes. At 15 minutes a large peak occurred at almost the same point as for HTPB/CLPS (i.e., an approximate average molecular weight of 142). At time of 17.5, 20.5, 23.5 and 26.5 minutes additional peaks occurred, followed by the typical HTPB peak at 30 minutes.

The HTPB/Diamantane did not have any distinct peak except at a time of 15 minutes and at approximately the end of the heating cycle. It started coming out at approximately 9 minutes from the injection, had its first peak at the same point as that of the HTPB/CLPS and HTPB/RJ-4 and its maximum peak almost at the end of the cycle.

3. High Heating Rate (Laser)

The gases emitted during the pyrolysis of the fuels using the laser beam (heating rate $7.3 \times 10^6 \frac{\text{Joules}}{\text{m}^2\text{-sec}}$) were withdrawn and injected into the gas chromatograph using again a gas tight syringe. The gas removal process probably resulted in a rapid chemical quench. However, future work should consider other gas sampling methods.

The results obtained for the four fuels investigated (PMM, HTPB/CLPS, HTPB/RJ-4 and HTPB/Diamantane) are shown in Figure 18. In the same figure the traces for the known standards (C_6H_{14}, C_7H_{16}, C_9H_{20}, $C_{10}H_{22}$ and $C_{12}H_{26}$) are also shown.

The PMM resulted in a small peak at an oven temperature of approximately 70°C and with a retention time of about 7 minutes. The small size of the peak was due to the small amount of sample that could be withdrawn. Comparing again the retention time of the PMM with that of Heptane (= 5 min, molecular weight of 100), it can be said that the average molecular weight of the gases emitted during the pyrolysis of PMM was approximately that of the monomer ($C_5H_8O_2$).

The HTPB/CLPS started coming out of the column at approximately 10.5 minutes. It had its maximum peak initially and from then on a distribution of molecular weights was obtained, with a small peak at about 30 minutes from the injection. The time at which the maximum peak occurred was a little less than that corresponding to the retention time of the nonane (C_9H_{20}), while the time of the later peak corresponded to the retention times of gases with molecular weights greater than that of Dodecane ($C_{12}H_{26}$).

The HTPB/RJ-4 started passing through the detector after approximately 10.5 minutes. It generally had the same pattern as that of HTPB/CLPS, with a peak at 11 minutes, corresponding to a retention time for gases having a molecular weight a little less than that of nonane. A distribution of molecular weights was then obtained until the end of the heating cycle.

The HTPB/Diamantane started coming out of the column at a time of approximately 10 minutes, corresponding to the retention time of gases with molecular weights between those of heptane and nonane. A distribution of molecular weights was then obtained. After approximately 18 minutes from injection (at an oven temperature of 140°C) a distinct peak occurred, corresponding to a gas with molecular weight almost that of dodecane. Then it gave a distribution of molecular weights up to the end of the cycle with a small distinct peak at a time of 27.5 minutes.

4. Summary of Results

It appears that the PMM always unzips to the monomer regardless of the heating rate (high or low) used during the pyrolysis. The thermograms of the HTPB based fuels indicated that gases with wide ranges of molecular weights were produced using both low (DTA) and high (laser) heating rates. The two heating rates produced almost the same pattern, giving a broad spectrum (distribution) of molecular weights with some distinct peaks corresponding mostly to molecular weights of nonane (128), decane (142) and dodecane (170).

C. FUEL COMPOSITION AND NEAR-WALL MIXING EFFECTS ON COMBUSTION EFFICIENCY

In this part of the investigation firings were made using HTPB/CLPS supplied by CSD (HTPB/CSD), HTPB supplied by NWC (HTPB/NWC), HTPB/RJ-4 and PMM. Results for the HTPB based fuels are presented in Table II and Figure 19.

TABLE II

RESULTS FROM FIRINGS WITH HTPB BASED FUELS

Run No.	Type of Fuel	$P_c * 10^{-3}$ (N/m^2)	$\dot{m}_p$ (kg/sec)	$\dot{m}_s$ (kg/sec)	L (m)	$\bar{r}$ (cm/sec)	$\frac{\eta_{\Delta T}}{\eta_{\Delta T_{max}}}$	ϕ
1	HTPB(CSD)	315.8	.248	-	.152	.0383	.92	.44
2		304.1	.120	.114	.229	.0264	.90	.47
3*		278.6	.238	-	.152	.0432	.59	.53
4	HTPB(NWC)	285.4	.251	-	.143	.0363	.84	.35
5		204.1	.086	-	.152	-	1.00	.56
6		224.8	.086	-	.152	-	.99	.71
7		362.0	.152	-	.152	-	.88	.62
8		376.5	.156	-	.152	-	.83	.68
9		262.0	.242	-	.152	-	.72	.33
10		273.7	.248	-	.152	-	.72	.36
11		310.3	.248	-	.229	-	.42	.92
12		395.1	.172	-	.229	-	.62	.80
13		382.7	.160	-	.229	-	.64	.86
14		296.7	.130	.102	.229	.0267	.91	.45
15*		284.1	.239	-	.152	.0400	.73	.45
16	HTPB/ RJ-4	303.4	.241	-	.152	.0440	.79	.50
17		313.7	.249	-	.147	.0440	.86	.46
18		342.7	.124	.113	.229	.0380	.84	.68
19*		310.6	.239	-	.152	.0554	.65	.67

* Grooved fuel surface (Fig. 2)

The combustion efficiency ($\eta_{\Delta T}$) of HTPB without bypass air increased significantly with decreasing equivalence ratio (ϕ) to $\phi \approx 0.4$ and then decreased (Fig. 19). The limited bypass data obtained at low values of ϕ indicated that bypass had little effect on $\eta_{\Delta T}$. Other reported data have shown that bypass can significantly increase $\eta_{\Delta T}$ for higher values of ϕ.

Past work at NPS and the results presented for PMM have shown that PMM generally has higher $\eta_{\Delta T}$ and that $\eta_{\Delta T}$ does not vary significantly with ϕ . As discussed above, the PMM tests were conducted at lower air mass flux than was HTPB. In discussions with Dr. Roger Dunlap at UTC/CSD he indicated (since the combustion process is dominated by diffusion processes) that fuel composition should not have much effect on $\eta_{\Delta T}$; also, that lower air mass flux should increase mixing and improve $\eta_{\Delta T}$. For these reasons two additional tests were conducted with HTPB at low air flow rates (Run Nos. 5 & 6, Table II). The low flow rate did result in very high $\eta_{\Delta T}$ and the limited data indicated that $\eta_{\Delta T}$ did not vary significantly with ϕ (similar to the behavior of PMM). The latter requires further experimental data for validation.

Enhanced near-wall mixing using a grooved fuel surface (Fig. 2) significantly increased the fuel regression rate and decreased $\eta_{\Delta T}$. Grooves have been found not to affect $\eta_{\Delta T}$ for PMM at low flow rates. The same may be true for HTPB. Apparently, at the high air flow rates, the surface grooves induced too much mixing in the flame region. Additional data are needed at lower air flow rates and with smaller/ fewer surface grooves.

The fuel consisting of HTPB/RJ-4 had lower $\eta_{\Delta T}$ than HTPB without bypass. Although based on limited data it appears that significantly different fuel properties may affect $\eta_{\Delta T}$. Turbulence/mixing can affect combustion if it alters the width of the flame region or the rate that fuel and oxygen are brought together. The HTPB/RJ-4 propellant did have a higher regression rate for the same air flow rate.

The limited data do not allow any strong conclusions to be drawn concerning the effects of fuel properties on the obtainable combustion efficiency. If there is an effect it does not appear to be a large one. However, near-wall mixing appears capable of affecting $\eta_{\Delta T}$ at high air flow rates. Much additional data are required.

D. THE EFFECTS OF BYPASS AIR, NEAR-WALL MIXING, AND EQUIVALENCE RATIO ON THE COMBUSTION EFFICIENCY OF PLEXIGLAS

The limited results obtained in Volume I indicated that induced mixing at the Plexiglas fuel surface had no significant effect on combustion efficiency at the flow rates investigated. In addition, the reduced combustion efficiency obtained with the use of bypass air could not be satisfactorily explained because data were taken with only one fuel grain length and one aft-mixing chamber geometry.

In this part of the investigation grain length was varied to effect changes in equivalence ratio for fixed air flow rates and circumferential grooves in the fuel grain were used to induce near-wall mixing. In addition, the length of the aft mixing chamber was varied to help determine the amount of combustion that occurs aft of the fuel grain.

Eighteen tests were conducted. The results are presented in Table III. A new lot of Plexiglas (PMM) was required for this study so that all test results could be meaningfully compared. The variation in combustion efficiency for different lots of Plexiglas has been observed before, and apparently results from variations in the curing process. The latter is thought to result in variations in residual monomer in the cured sheets of Plexiglas.

The results in Fig. 20 indicate that efficiencies of approximately 100% were achieved without bypass, independent of ϕ . As discussed above

TABLE III

RESULTS FROM PMM TESTS

Run No.	Config*	$P_c * 10^{-3}$ (N/m^2)	$\dot{m}_p$ (kg/sec)	$\dot{m}_s$ (kg/sec)	L (cm)	ϕ	$\bar{r}$ (cm/sec)	$\eta_{\Delta T}$
1	NBP	406.1	.093	0	30.5	.74	.0163	1.02
2	NBP	419.9	.088	0	35.6	.85	.0145	1.06
3	NBP	439.2	.090	0	40.6	.98	.0155	.99
4	NBP	458.5	.093	0	45.7	1.06	.0152	1.03
5	BP	333.0	.044	.040	35.6	.91	.0150	.82
6	BP	368.9	.046	.041	45.7	.95	.0132	.79
7	BP	393.8	.046	.041	55.9	1.34	.0147	.93
8	BP	379.2	.047	.042	61.0	1.34	.0137	.82
9	NBP-G	368.9	.091	0	20.3	.62	.0188	1.00
10	NBP-G	431.6	.090	0	27.9	.90	.0211	.99
11	BP	390.9	.047	.044	53.3	1.17	.0140	.76
12	BP	378.5	.046	.041	50.8	1.03	.0130	.76
13	BP	368.2	.044	.042	48.3	1.06	.0137	.73
14	BP	376.5	.046	.042	35.6	.79	.0109	.93
15	BP	355.1	.045	.043	35.6	.65	.0119	.95
16	BP	366.8	.045	.043	35.6	.67	.0099	1.00
17	NBP-SMC	406.1	.089	0	35.6	.88	.0157	.94
18	NBP-SMC	419.9	.088	0	35.6	1.05	.0147	.97

* NBP = non bypass, BP = 50/50 bypass, SMC = shortened aft mixing chamber, G = Grooved Fuel

this may be due in part to the low air flow rates which were used. However, lower efficiencies have been obtained at the same flow rates from other lots of Plexiglas [Refs. 7 & 8].

Grains with grooved surfaces (Fig. 2) were tested to supplement the earlier data obtained to investigate the effects of enhanced near-wall mixing. In these tests grain length was varied to obtain ϕ's over the same range as tested without the grooves. The results (Fig. 20) again indicated that $\eta_{\Delta T}$ was not significantly affected and that the regression rate was increased (Table III).

For the bypass configuration the combustion efficiencies were 22 to 28 points lower than the combustion efficiencies of the non-bypass configured fuel grains (Fig. 20). The combustion efficiencies with bypass appeared to behave more like HTPB, i.e., a minimum $\eta_{\Delta T}$ near $\phi = 1.0$.

The decrease in combustion efficiency with bypass noted above can result from the bypass air quenching the reaction in the aft mixing chamber and/or by affecting changes upstream within the fuel grain. In order to clarify this behavior, tests were conducted without bypass with a shortened aft mixing chamber (experiments 17 and 18, Table III). Experiment 18 used the same fuel grain that was used in experiment 17. With a much shorter aft mixing chamber (approximately 88% less volume than all previous runs, L/D = .35) there was a 7-8% loss in combustion efficiency when compared to similar non-bypass configured grains with a full sized mixing chamber (Fig. 20). These results indicate that approximately 7-8% of the combustion process takes place in the full sized aft mixing chamber (L/D = 2.93) without bypass. Assuming a similar behavior with bypass, the remaining 15-20% loss in efficiency when bypass was used apparently resulted from changes in the combustion process within the fuel grain.

In a concurrent and related area of research, pressure oscillations (instabilities in the combustion process) were observed to be occurring in the experiments with the bypass configured fuel grains. In an effort to isolate the sources of the instabilities both the primary and bypass air flows were choked at the motor inlets for experiments 14, 15 and 16. Choking of the inlets did enable the combustion to occur under stable conditions. Figure 20 shows that the combustion efficiency for these three experiments increased 15-20 points over the bypass configured experiments with combustion instabilities. However, the instabilities increased the fuel regression rate and increased ϕ for the same grain lengths. It

is not clear at this point whether or not the instabilities reduced $\eta_{\Delta T}$. However, even though the bypass configuration can be made to operate with stable combustion, the bypass air still adversely affected 7-8% of the combustion process; most probably by quenching the combustion process occurring in the aft mixing chamber. Apparently, the unburned hydrocarbons/carbon leaving the fuel grain burn most efficiently for PMM fuel when allowed to react more slowly in the aft mixing chamber.

VI. CONCLUSIONS

1. Combustion is approximately 92% complete within the fuel port of PMM grains when burned at low air flow rates. The remaining 8% is often achieved in the aft mixing chamber without bypass air. For these conditions bypass air apparently quenches chemical reactions, reducing the efficiency by 8%.

2. Bypass air can significantly affect the combustion process within the fuel port. With PMM grains, combustion instability significantly increases the fuel regression rate.

3. Variation in fuel properties does appear to affect the obtainable $\eta_{\Delta T}$ but the differences are not large.

4. PMM unzips to a monomer at both high and low heating rates whereas HTPB releases hydrocarbons with a very broad spectrum of molecular weights. Below 500°C PMM has a dominant endothermic reaction whereas HTPB has a dominant exothermic reaction.

5. All combustion instabilities observed to date have been at low frequency and have resulted from a coupling with the inlet air feed system.

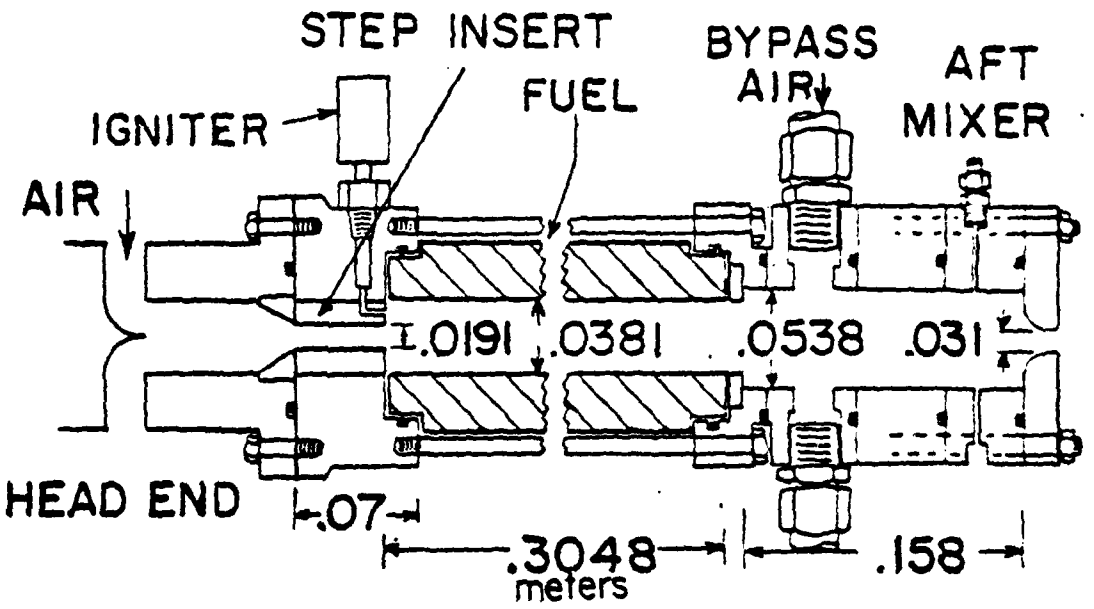

Fig. 1. Schematic of Solid Fuel Ramjet Apparatus

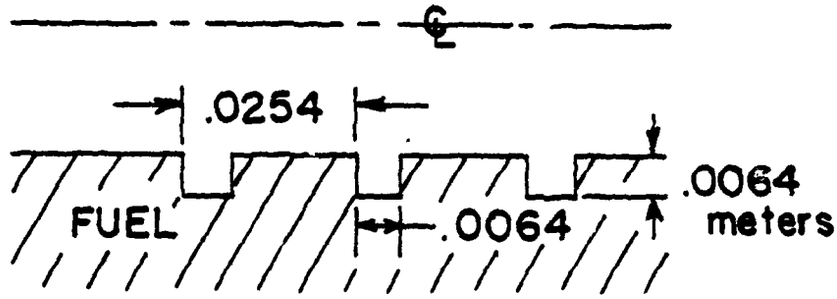

Fig. 2. Schematic of Fuel Grain with Grooved Surface

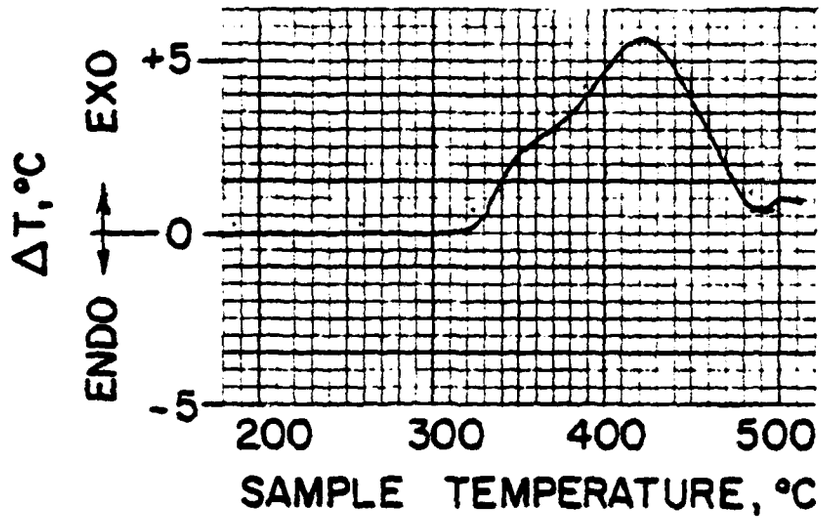

Fig. 3. DTA Results for HTPB/CLPS Fuel

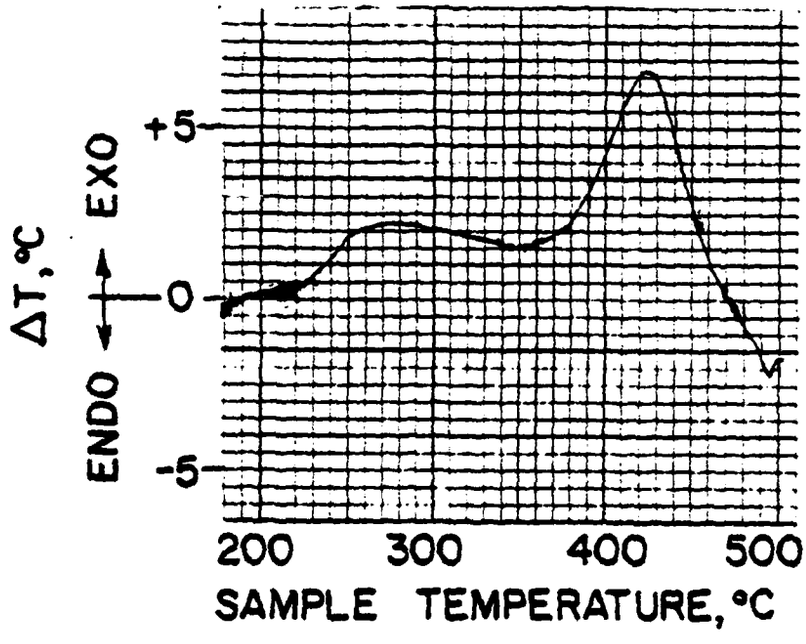

Fig. 4. DTA Results for R-45M with AO

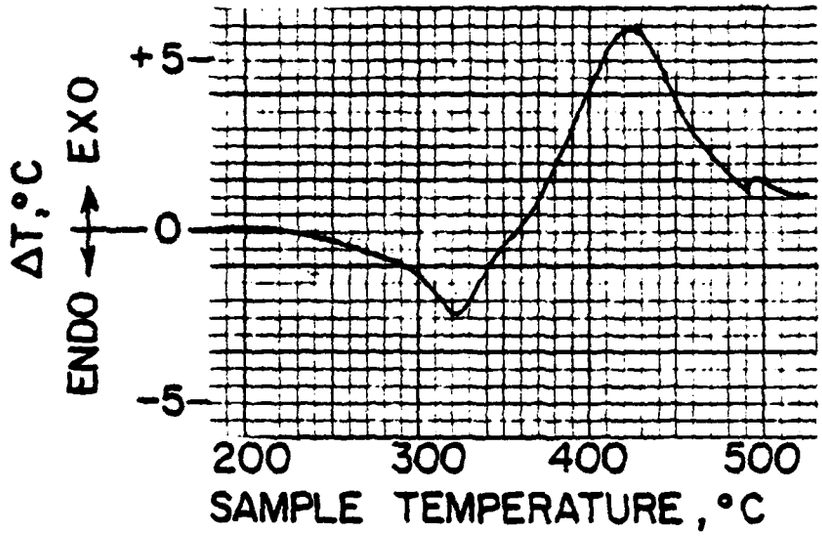

Fig. 5. DTA Results for HTPB/Binor-S Fuel

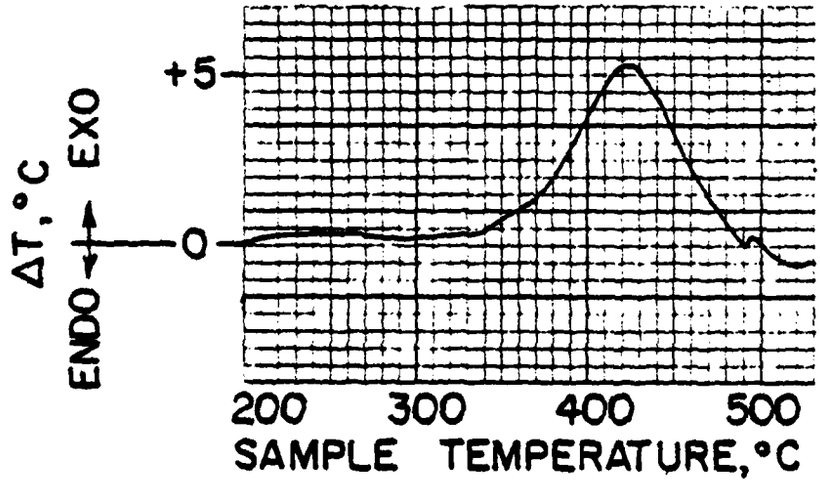

Fig. 6. DTA Results for HTPB/Magnesium Fuel

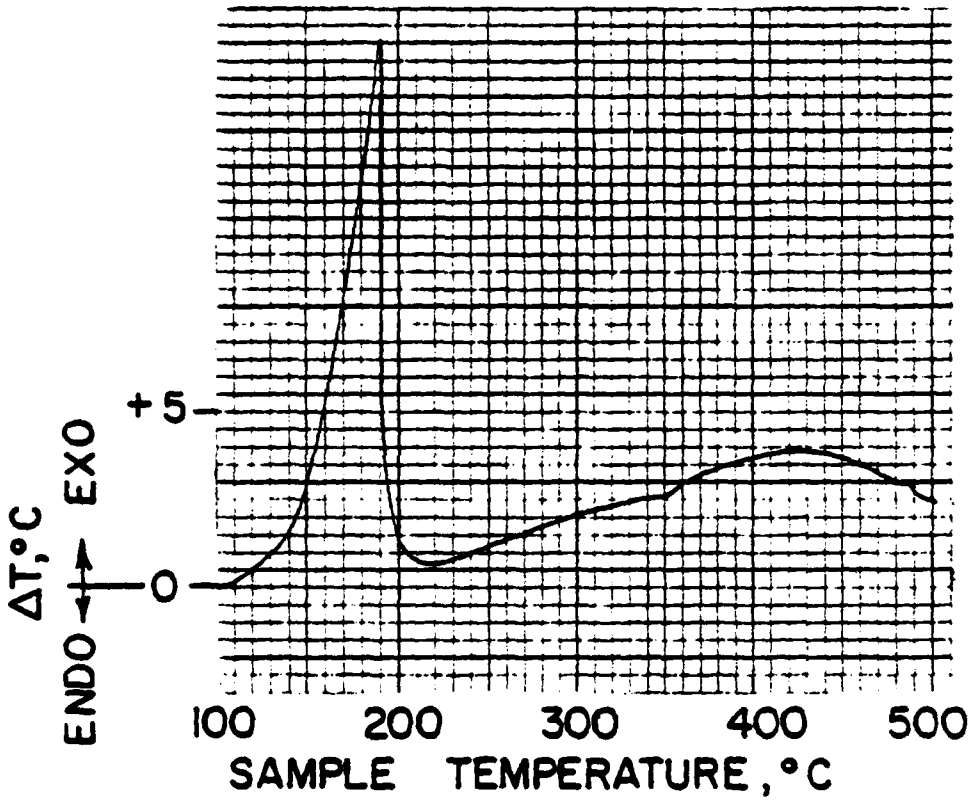

Fig. 7. DTA Results for HTPB/RJ-4 Fuel

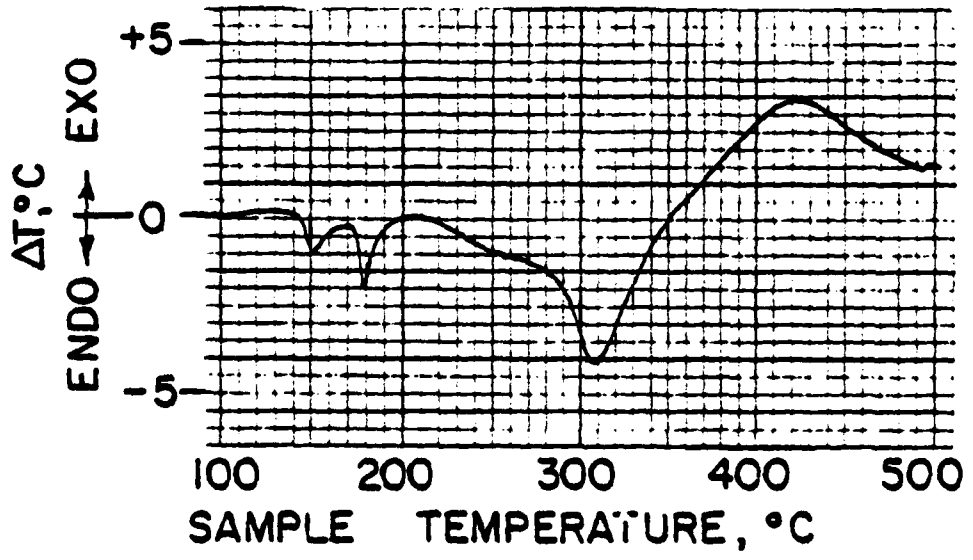

Fig. 8. DTA Results for HTPB/Diamantane Fuel

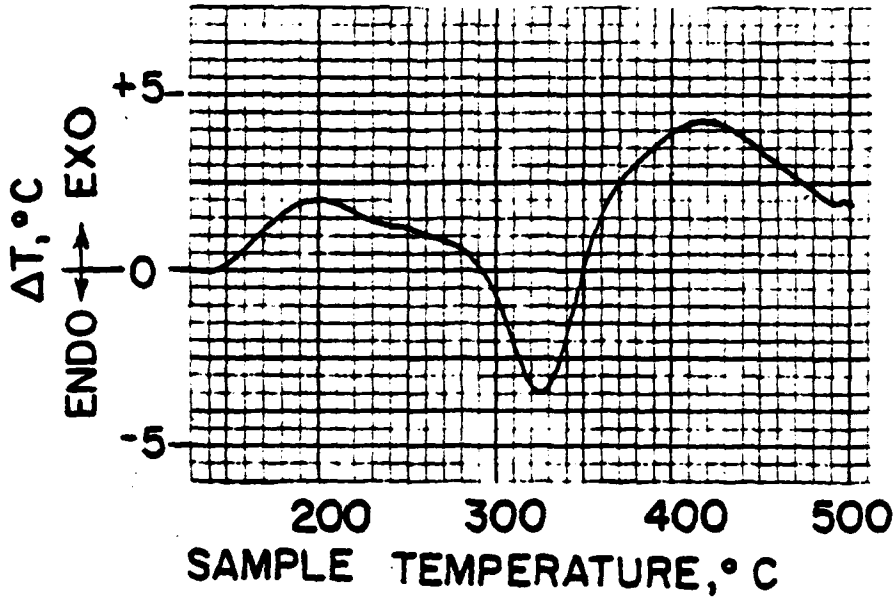

Fig. 9. DTA Results for HTPB/CPD Oligomers Fuel

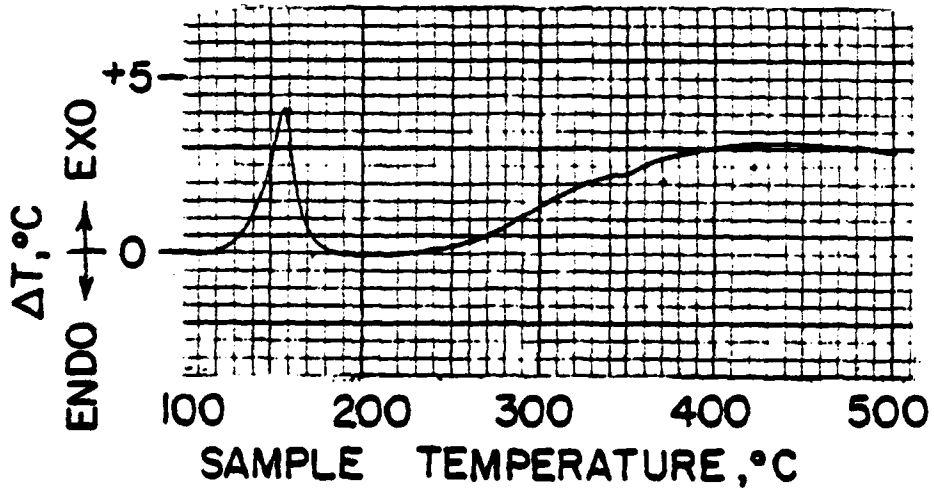

Fig. 10. DTA Results for HTPB/RJ-5-B/RJ-4 Fuel

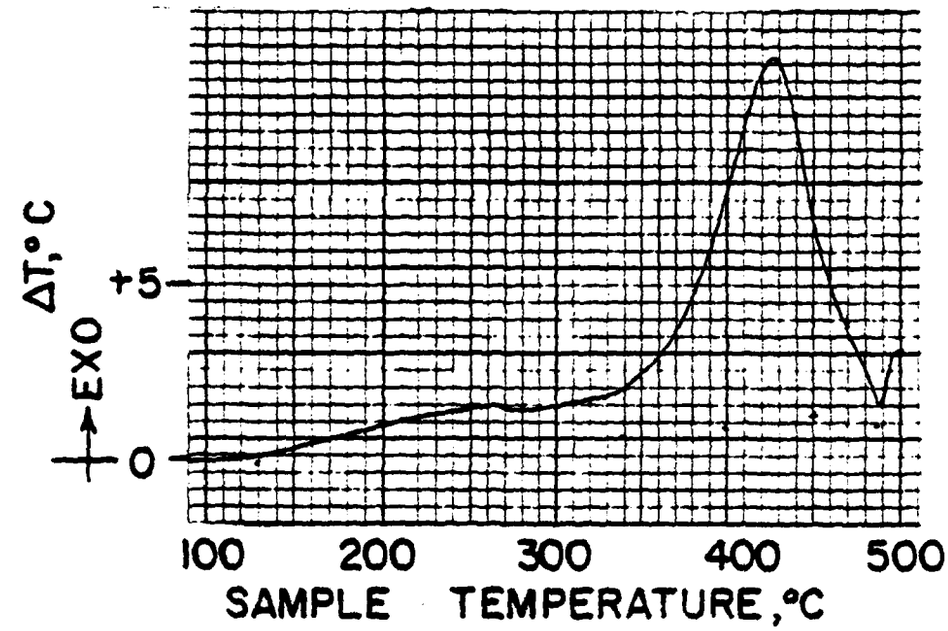

Fig. 11. DTA Results for R45 HT/DDI Fuel

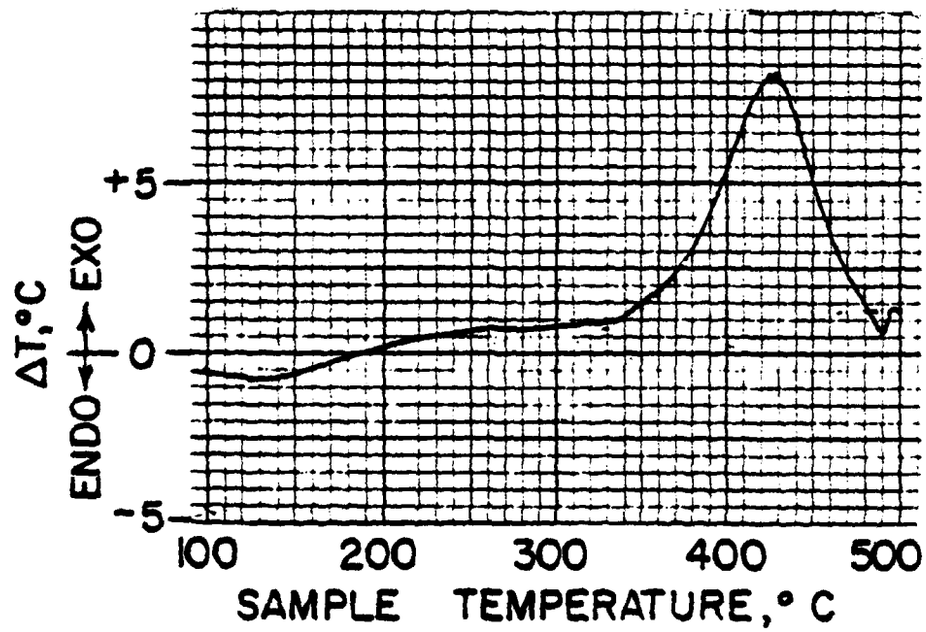

Fig. 12. DTA Results for R45 M/DDI Fuel

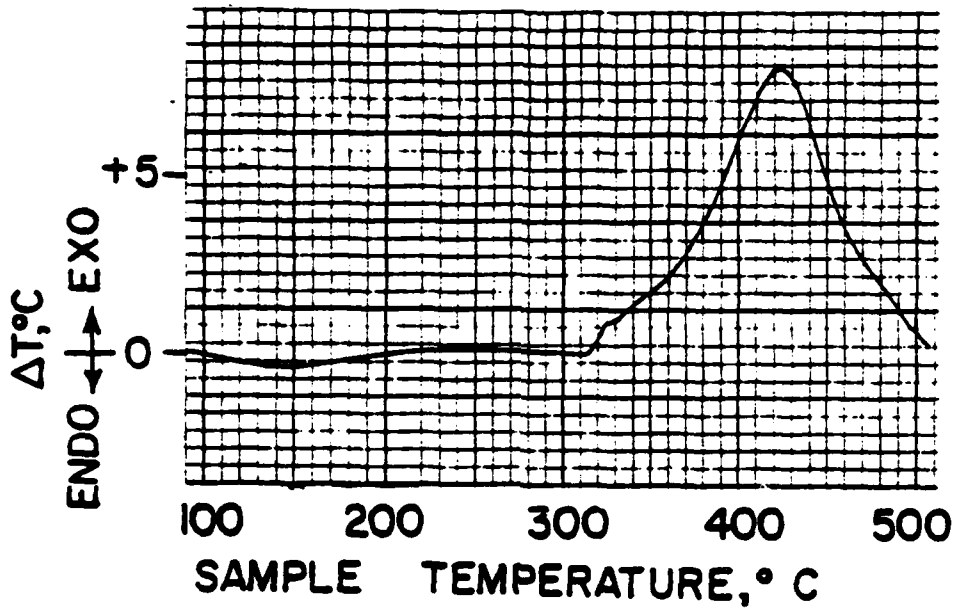

Fig. 13. DTA Results for R45M/TDI Fuel

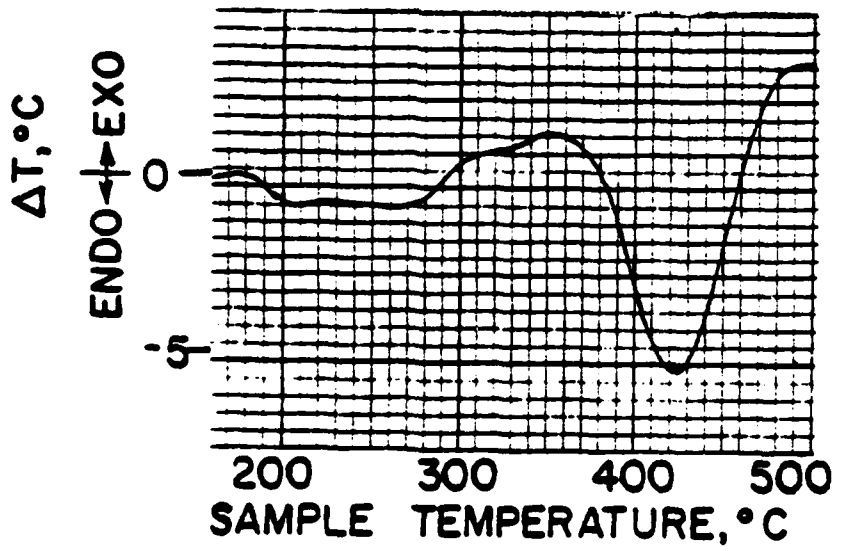

Fig. 14. DTA Results for DMM Fuel

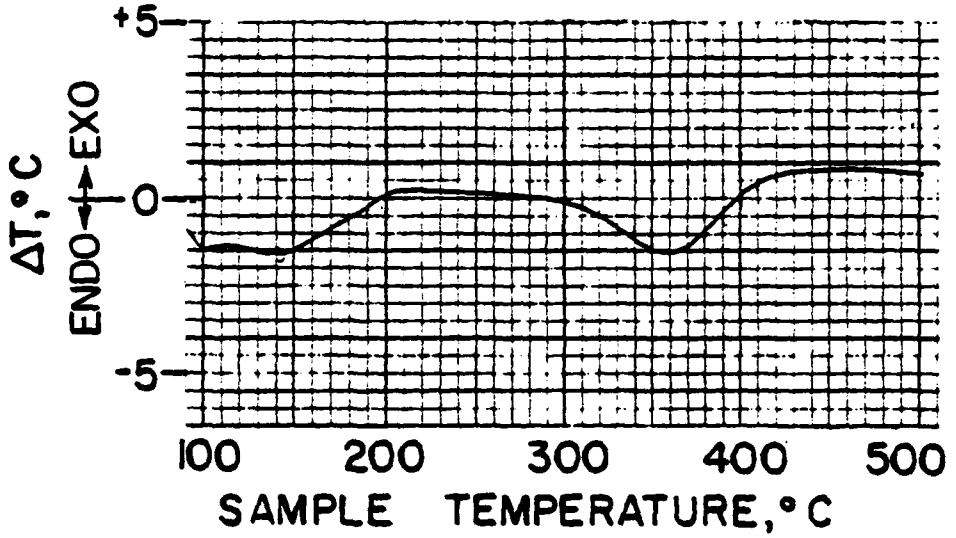

Fig. 15. DTA Results for Uncured Zecorez Fuel

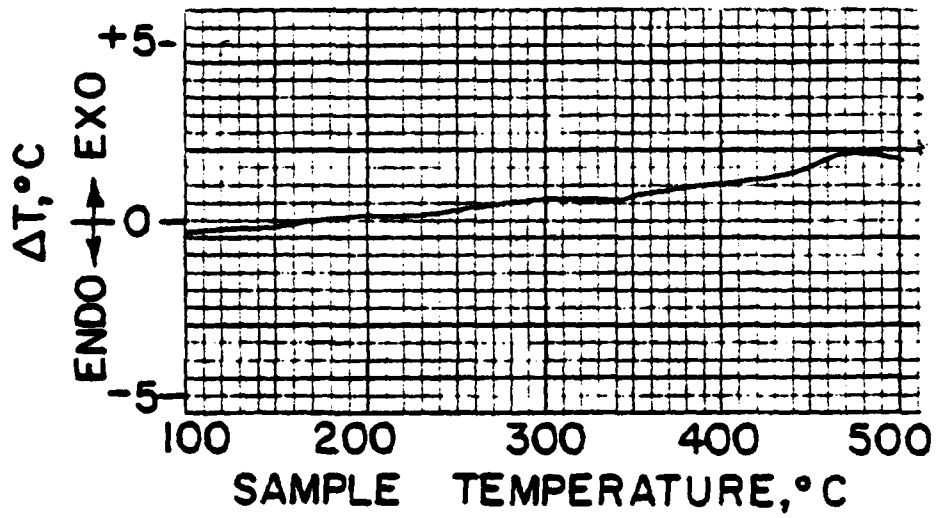

Fig. 16. DTA Results for the Cured Zecorez Fuel

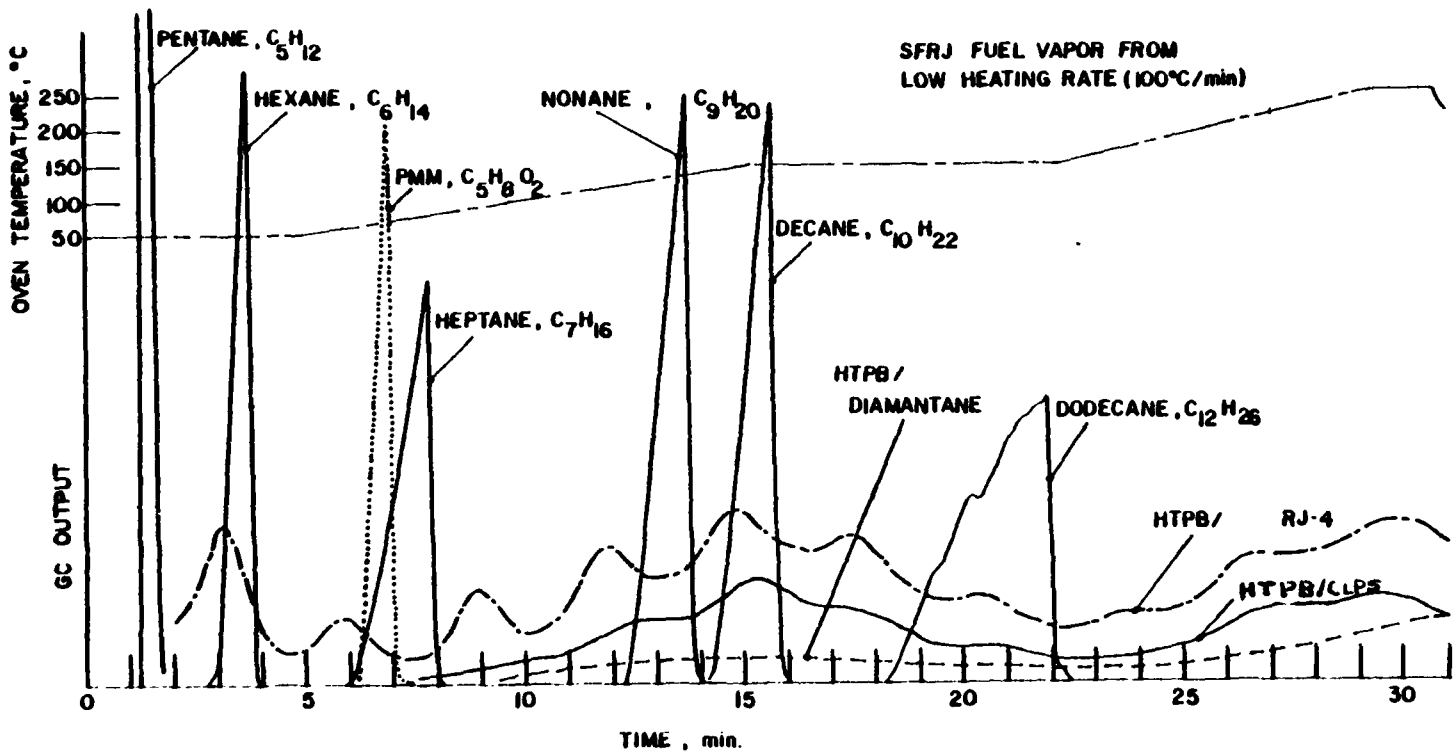

Fig. 17. Gas Chromatograph Results Obtained with Low Heating Rate

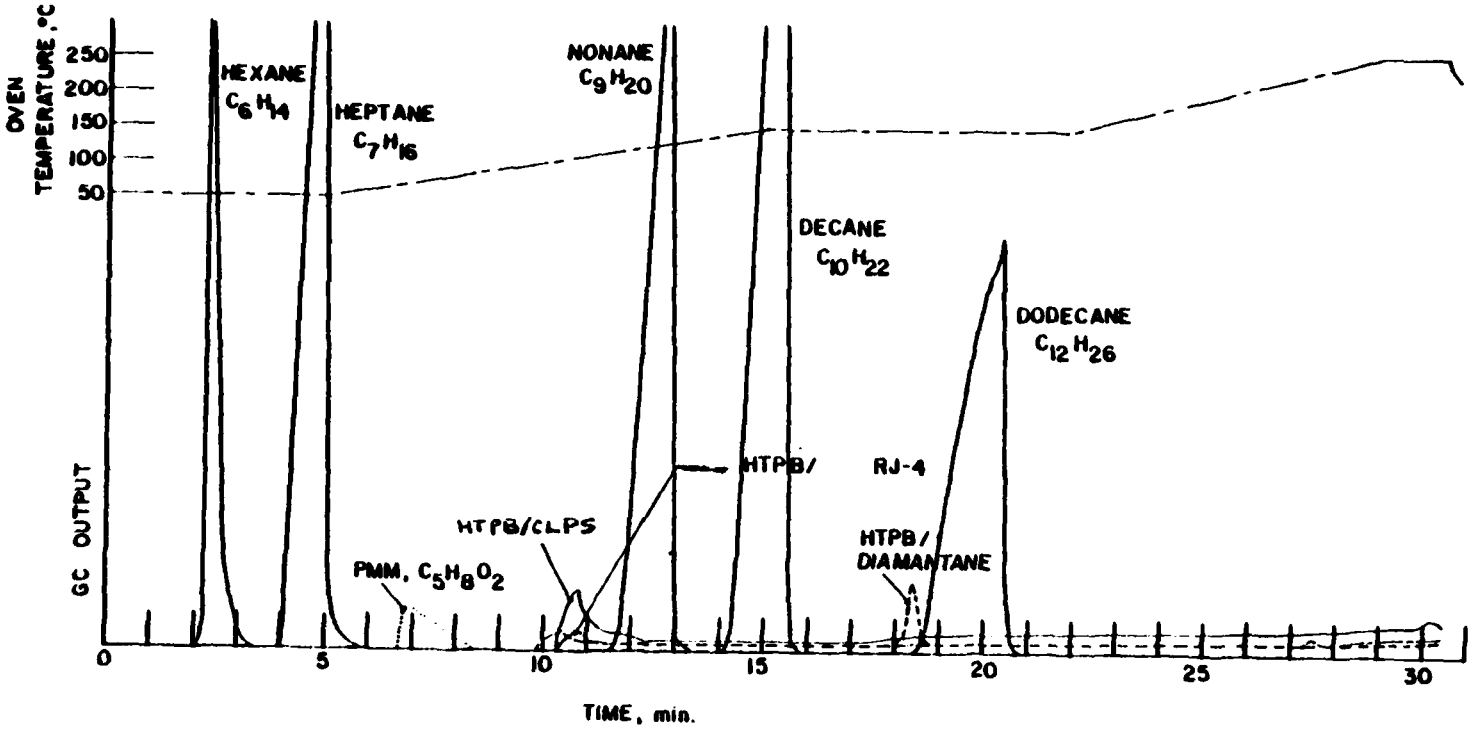

Fig. 18. Gas Chromatograph Results Obtained with High Heating Rate

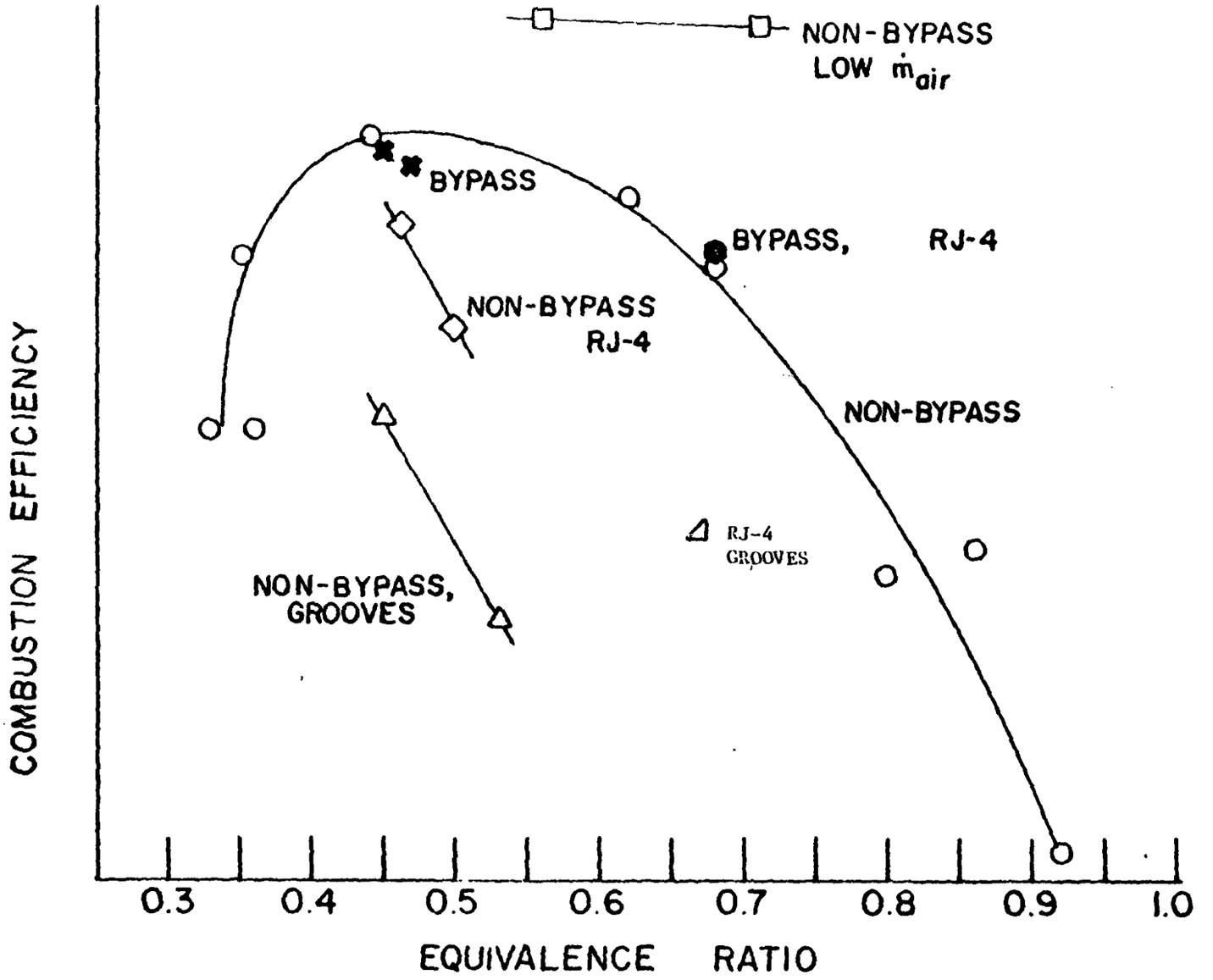

Fig. 19. Combustion Efficiency of HTPB Based Fuels

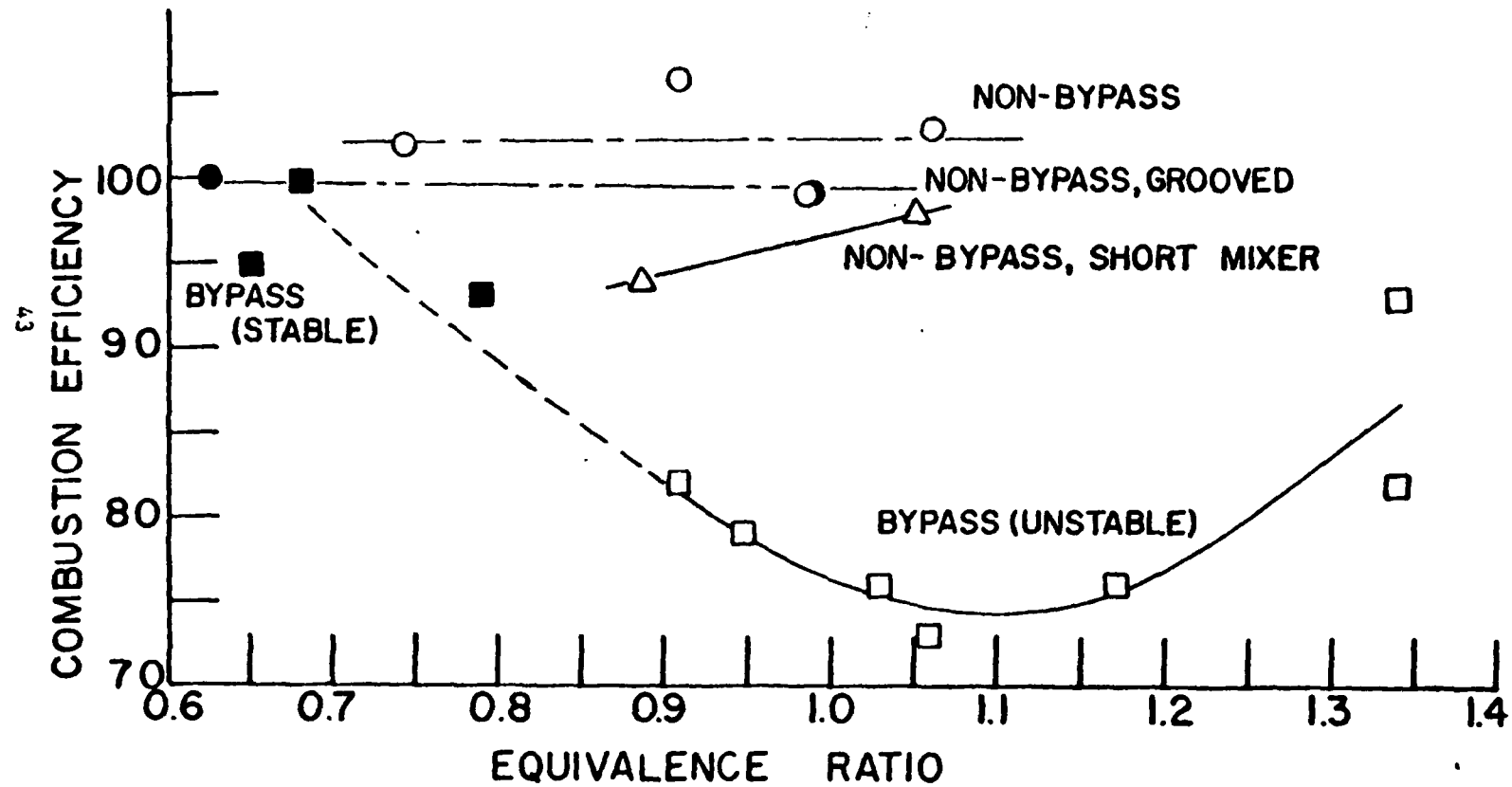

Fig. 20. Combustion Efficiency of PMM Fuel

VII. REFERENCES

1. Netzer, D. W., "Modeling Solid-Fuel Ramjet Combustion," JSR, Vol. 14, No. 12, Dec. 1977, pp. 762-766.

2. Netzer, D. W., "Model Applications to Solid-Fuel Ramjet Combustion," JSR, Vol. 15, Sept-Oct. 1978, pp. 263-264.

3. Stevenson, C. A. and Netzer, D. W., "Primitive-Variable Model Applications to Solid Fuel Ramjet Combustion," JSR, Vol. 18, No. 1, Jan-Feb., 1981, pp. 89-94.

4. Boaz, L. D. and Netzer, D. W., "An Investigation of the Internal Ballistics of Solid Fuel Ramjets," NPS Report NPS-57Nt73031A, March 1973.

5. Phaneuf, Jr., J. T. and Netzer, D. W., "Flow Characteristics in Solid Fuel Ramjets," NPS Report NPS-57Nt74081, May 1974.

6. Mady, C. J., Hickey, P. J., and Netzer, D. W., "An Investigation of the Combustion Behavior of Solid Fuel Ramjets," NPS Report NPS-67Nt77092, Sep. 1977.

7. Mady, C. J., Hickey, P. J., and Netzer, D. W., "Combustion Behavior of Solid Fuel Ramjets," JSR, Vol. 15, No. 3, May-June 1978, pp. 131-132.

8. Hewett, M. E. and Netzer, D. W., "Application of Light Extinction Measurements to the Study of Combustion in Solid Fuel Ramjets," NPS Report NPS-67-78-008, Nov. 1978.

9. Hewett, M. E. and Netzer, D. W., "Light Transmissio Measurements in Solid Fuel Ramjet Combustors," JSR, Vol. 18, No. 2, March-April 1981, pp. 127-132.

10. Burdette, W. and Reed, R., Jr., "Navy High Energy Solid Ramjet Fuel Program," 1979 JANNAF Propulsion Meeting, Anaheim, CA, 5-9 March 1979.

11. Schadow, K. C., "Solid Fuel Ramjet Evaluation," 16th JANNAF Combustion Meeting, Monterey, CA, 10-14 Sep. 1979.

12. Gary, P. D., Thermoanalytical Methods of Investigation, Academic Press, Inc., 1965.

13. Mackenzie, R. C., Differential Thermal Analysis, Vol. I and II, Academic Press, Inc., 1973.

14. Wendlandt, W. W., Thermal Methods of Analysis, Interscience Publishers, 1964.

INITIAL DISTRIBUTION LIST

	No. of Copies
1. Library, Code 0212	2
Dean of Research, Code 012	2
Naval Postgraduate School	
Monterey, CA 93940	
2. Department of Aeronautics	
Code 67	
Naval Postgraduate School	
Monterey, CA 93940	
Prof. M. F. Platzer, Chairman	1
Prof. D. W. Netzer	10
M. Metochianakis	2
W. Goodwin	2
U. Katz	2
3. Defense Technical Information Center	2
Attn: DDC-TCA	
Cameron Station, Bldg. 5	
Alexandria, VA 22314	
4. Naval Air Systems Command	2
Washington, D.C. 20361	
AIR-330	
5. Naval Weapons Center	
China Lake, CA 93555	
Tech. Library, Code 753	3
F. Zarlingo, Code 3246	3
K. Schadow, Code 388	1
W. Burdette, Code 3244	1
6. Chemical Systems Division	
United Technologies	
P. O. Box 358	
Sunnyvale, CA 94088	
Tech. Library	1
R. Dunlap	1
A. Holzman	1
G. Jensen	1
P. Willoughby	1
P. LaForce	1
7. Chemical Propulsion Information Agency	2
APL-JHU	
Johns Hopkins Road	
Laurel, MD 20810	
8. AFAPL	
Wright-Patterson AFB, OH 45433	
R. D. Stull	2